

Cite this article as: Tian Qinghua, Hu Zhixiang, He Zhiqiang, et al. Preparation of 7N High-Purity Indium by Vacuum Distillation-Zone Refining Combination[J]. Rare Metal Materials and Engineering, 2025, 54(08): 1947-1955. DOI: <https://doi.org/10.12442/j.issn.1002-185X.20240439>.

ARTICLE

Preparation of 7N High-Purity Indium by Vacuum Distillation-Zone Refining Combination

Tian Qinghua¹, Hu Zhixiang^{1,2}, He Zhiqiang¹, Guo Xueyi¹, Zhu Liu², Xu Zhipeng¹

¹ School of Metallurgy and Environment, Central South University, Changsha 410083, China; ² Vital Materials Co., Ltd, Qingyuan 511500, China

Abstract: High-purity indium finds extensive application in the aerospace, electronics, medical, energy, and national defense sectors. Its purity and impurity contents significantly influence its performance in these applications. High-purity indium was prepared by combining zone refining with vacuum distillation. Results show that the average removal efficiency of impurity Sb can approach 95%, while the removal efficiency of impurities Sn and Bi can reach over 95%, and the removal efficiency of Si, Fe, Ni, and Pb can reach over 85%. Ultimately, the amount of Sn and Sb impurities is reduced to 2.0 and 4.1 $\mu\text{g}/\text{kg}$, respectively, and that of most impurities, including Fe, Ni, Pb, and Bi, is reduced to levels below the instrumental detection limit. The average impurity removal efficiency is 90.9%, and the indium purity reaches 7N9.

Key words: indium; high-purity; vacuum distillation; zone refining

1 Introduction

Indium demonstrates exceptional properties, including high ductility, plasticity, corrosion resistance, and superior light permeability and electrical conductivity, thus finding extensive applications in critical sectors such as aerospace, electronics, medicine, defense, and energy^[1-4]. High-purity indium is commonly used in the production of indium tin oxide targets^[5-6], CuInGaSe, CuInSe₂ thin-film solar cells^[7], as well as other semiconductor compounds such as InSb, InAs^[8], and InP^[9]. In recent years, there has been a dramatic increase in the demand for high-purity indium not only for high-end technologies, but also for the purity itself, as even ppm-level impurities can affect the electron transfer behavior of electronic devices^[10]. With the rapid development of microelectronics, semiconductors, and other cutting-edge technologies, efficient purification methods have received more attention than ever before^[11-12].

The purification of indium using the vacuum distillation technique has received wide attention from researchers^[13-15]. Using vacuum distillation, Lei et al^[16] obtained indium with a purity of 99.99% by controlling the distillation and conden-

sation temperatures. Zhu et al^[17] purified raw indium from 2N grade (99wt%) to 4N5 grade (99.995wt%), firstly removed low-boiling point impurities such as cadmium, zinc, and lead, and then eliminated high-boiling point impurities such as copper and iron through second-stage vacuum distillation. Zhang et al^[18] obtained refined indium with a purity of 4N by vacuum distillation and graded condensation, with a recovery more than 90.57%. Researchers generally use vacuum distillation to prepare indium with a purity of 5N and below, and less attention has been paid to the preparation of high-purity indium by vacuum distillation. Given the challenges associated with purifying indium to 6N purity level or higher using vacuum distillation alone, zone refining has emerged as a widely recognized technique for preparing ultrahigh-purity indium.

Many researchers have explored the solute removal and optimization of processing parameters during zone refining^[19-23]. Wu et al^[24] purified 5N indium to 6N grade by zone refining; during the experiment, several zone refining passes were carried out for better removal of impurity elements with equilibrium distribution coefficients close to 1,

Received date: July 18, 2024

Foundation item: National Key Research and Development Program of China (2023YFC2907904); National Natural Science Foundation of China (52374364)
Corresponding author: Xu Zhipeng, Ph. D., Professor, School of Metallurgy and Environment, Central South University, Changsha 410083, P. R. China, E-mail: zhipeng.xu@csu.edu.cn

Copyright © 2025, Northwest Institute for Nonferrous Metal Research. Published by Science Press. All rights reserved.

and the production efficiency was drastically reduced. Prasad^[25] and Munirathnam^[26] et al investigated the effect of varying the number of zone refining passes, zone width, and melting zone travel speed on the impurity removal efficiency in the process of refining tellurium (Te) and found that a moving speed of $30 \text{ mm}\cdot\text{h}^{-1}$ could significantly separate impurities. The zone refining technique can be applied to the preparation process of ultrahigh-purity metals, but the purification efficiency is low. In this research, a combination of vacuum distillation and zone refining was used to prepare high-purity indium. Firstly, vacuum distillation was used to remove the impurities in indium initially. Then, zone refining technique was used to remove the trace impurities in depth further to prepare high-purity indium. In addition, it was found that the content of impurity antimony was still high after the combination of vacuum distillation and zone refining. Therefore, hydrogenation technique was applied to remove the impurity antimony further to realize the preparation of 7N high-purity indium.

2 Results and Discussion

2.1 Theory

2.1.1 Vacuum distillation

Vacuum distillation technique has the advantages of non-pollution, high efficiency, and high recovery rate, and is widely used in the separation and purification of alloys as well as the refining and purification process of crude metals^[27-28]. By controlling the distillation temperature, condensation temperature, distillation time, vacuum conditions, etc, the impurity elements are selectively volatilized in the vacuum distillation process, and the volatiles are condensed at different locations, which makes the impurities and the primary metal effectively separated. Thus, the purpose of purifying the primary metal is achieved. The basic principle of vacuum distillation was to utilize the difference in vapor pressure of different metals for purification. In the purification of indium using vacuum distillation, indium was more volatile during the distillation process because of its higher vapor pressure. Segmented condensation collection was used to obtain high-purity indium, while low-volatile impurities were left in the distillation residue, and high-volatile impurities were condensed at the upper end of the collection. The vapor pressure of indium, P (Pa), was related to the temperature, T , as shown by Eq.(1)^[29-30]:

$$\lg P = AT^{-1} + b \lg T + CT + D \quad (1)$$

where P denotes the vapor pressure of the pure metal; T denotes the temperature; A , B , C , and D denote constants.

The horizontal distillation furnace was used in the experiment, and the principle of sub-condensation of impurities in the distillation process is shown in Fig.1. Firstly, the saturated vapor pressures of the impurities in indium were calculated and analyzed. The saturated vapor pressure of pure elements in indium raw material decreases in the order of $\text{P} > \text{S} > \text{Cd} > \text{Zn} > \text{Mg} > \text{Sb} > \text{Bi} > \text{Pb} > \text{In} > \text{Ag} > \text{Sn} > \text{Cu} > \text{Fe} > \text{Ni} > \text{Si}$. When the system pressure is 10^{-2} Pa and the distillation temperature

is $1000-1100$ °C, impurities such as P, S, Zn, Mg, and Sb evaporate into the gas phase due to the high saturation vapor pressure, and impurities such as Sn, Cu, Fe, Ni, and Si remain in the liquid phase. Therefore, it is appropriate to set the distillation temperature to $1000-1100$ °C during the experiment. Furthermore, since the saturation vapor pressure of impurities Sb, Bi, Pb, Sn, etc in indium was close to the saturation vapor pressure of indium, it was difficult to remove these impurities in the process of indium vacuum distillation and purification. To effectively separate the impurities Sb, Bi, Pb, and Sn from the main metal indium, two temperature control sections were used in the experimental process. The temperature of the condensation section was controlled to be $800-900$ °C, so the volatiles could be fully condensed in the condensation section to improve the removal efficiency of the impurities. As shown in Fig. 1, the temperature in the distillation furnace gradually decreases from left to right; the first temperature is the distillation temperature, and the second temperature is the condensation temperature.

There are two drawbacks in the purification of indium metal by vacuum distillation: one is that it is difficult to remove the impurity elements such as Si, Fe, and Sb, which are similar to indium in the vapor pressure, and the other is that the recovery rate will be drastically reduced if we want to obtain with higher purity. Thus, it is difficult to obtain indium with higher purity indium by vacuum distillation alone. Compared to vacuum distillation, zone refining is a deep purification technique that can effectively produce high-purity indium with a purity of 7N and above.

2.1.2 Zone refining

In the early 1950s, Pfann^[31-32] firstly proposed the zone refining purification method. Zone refining was to take advantage of the difference in solubility of impurities in the liquid and solid phases of the host metal to purify the metal. The purification of the host metal is achieved by localized melting of metal rods by heating, while controlling the directional movement of the melting zone to precipitate impurities and to change their distribution^[33]. Zone refining has basically the same principle as the polarization method and directional solidification^[32,34-36]. The ratio of the concentration of impurities in the solid phase (C_s) to the concentration in the liquid phase (C_l) was defined as the equilibrium distribution coefficient k_0 ($k_0 = C_s/C_l$). Many factors affected the purification effect of zone refining, such as the equilibrium distribution coefficient k_0 , the travel speed of the melting zone, and the number of zone refining passes. Researchers have proposed the effective distribution coefficient (k_{eff}), and the relationship between k_{eff} and k_0 can be expressed as follows^[37]:

$$k_{\text{eff}} = \frac{k_0}{k_0 + (1 - k_0) \exp(-v\delta/D)} \quad (2)$$

where D is the impurity diffusion coefficient in the melt, δ is the thickness of the diffusion layer adjacent to the solidification interface, and v is the travelling speed in the molten zone.

The distribution coefficients of the main impurities in

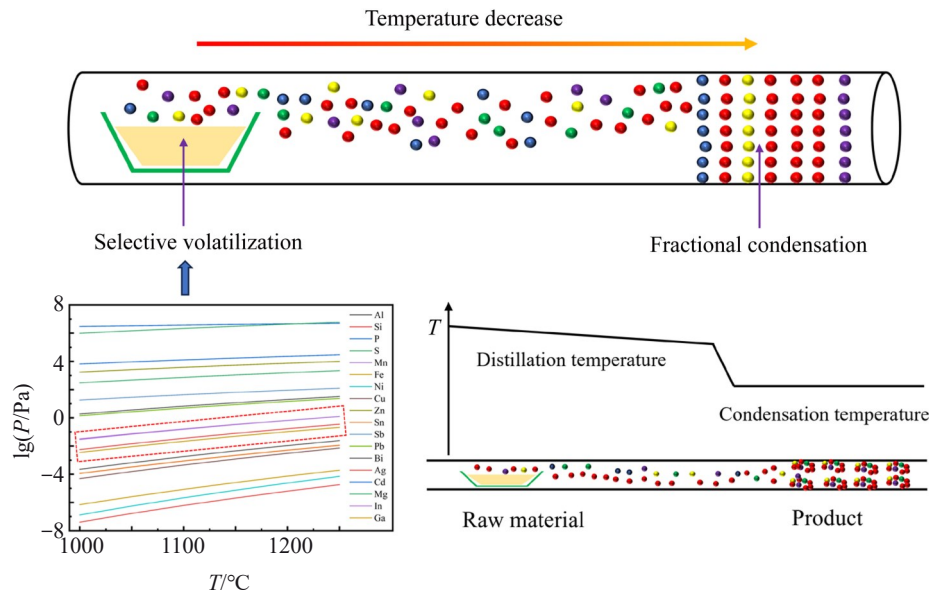


Fig.1 Schematic diagrams of vacuum distillation

indium are shown in Table 1^[38], from which it can be analyzed that the distribution coefficients of the impurities Tl, Pb, Mg, Sn, and Cd in indium are close to 1, so it is more difficult to be removed in the zone refining process.

Compared with other methods, zone refining has the advantages of high purification limit, no environmental pollution during the experimental process, and simple operation^[39]. In the zone refining process, the distribution of impurities in the ideal state is shown in Fig.2^[40], when $k_{\text{eff}} > 1$ for the impurity, the solubility of impurities in the solid phase is greater than that in the liquid phase, and the impurities are enriched toward the solid phase region, as shown in Fig.2a. The figure is divided into three regions: the upper part represents the liquid phase region, the middle part is the liquid-solid equilibrium region, and the lower part is the solid phase region. Conversely, when $k_{\text{eff}} < 1$ for the impurity, the solubility

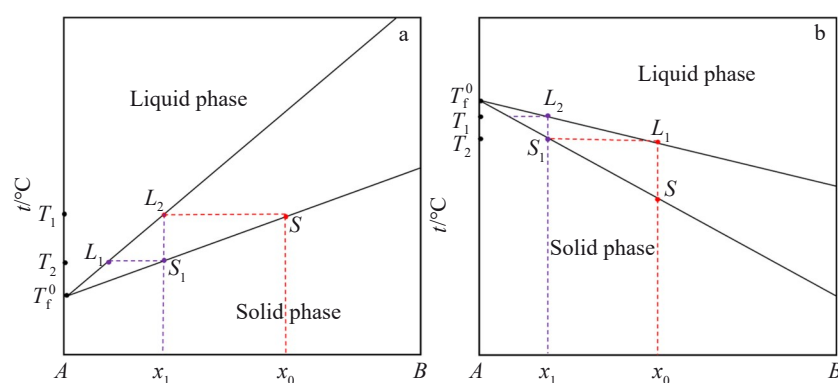
of the impurity in the solid phase is less than that in the liquid phase, and the impurity is enriched toward the liquid phase region, as shown in Fig.2b.

In this experiment, four melting zones were used for the zone refining of indium, and the schematic diagram is shown in Fig.3. Implementing multiple melting zones in zone refining can significantly enhance purification efficiency and reduce the experimental duration. After multiple passes of zone refining, the impurities were enriched at the first and last ends of the metal rods. The impurity-enriched areas at both ends are removed, and the middle part is the high-purity product. For example, most impurities, such as Al, Si, Fe, Cu, Ni, and Sn, migrate to the tail end of the indium rods, and impurities such as Pb and Mg migrate to the head end of the indium rods.

After zone refining, the content of most impurities, such as Si, Fe, and Sb, in indium metal can be reduced. After that, the

Table 1 Distribution coefficient k_0 of impurities in the indium^[38]

Al	Si	Cd	S	Mn	Fe	Mg	Ni	Cu	Zn	Sn	Tl	Pb	Ag
<1	<0.1	0.67–0.72	<0.1	<0.5	<0.1	1.33–1.77	0.01–0.06	0.06–0.08	0.36–0.43	0.73–0.8	≈1	1–1.07	0.06–0.09

Fig.2 Ideal binary distribution graphs^[40]: (a) $k_{\text{eff}} > 1$ and (b) $k_{\text{eff}} < 1$

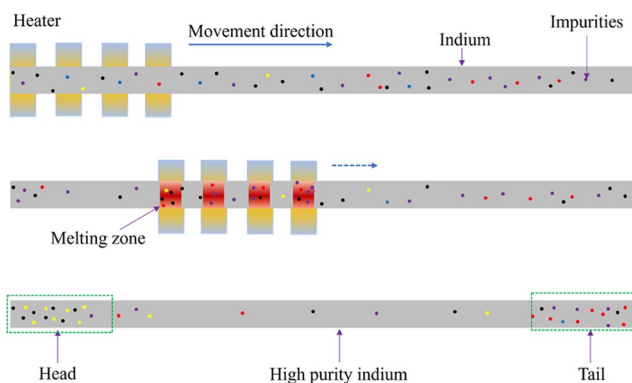


Fig.3 Schematic diagram of zone refining

purified indium is loaded into a graphite boat for hydrogenation and ingot casting to obtain 7N high-purity indium products.

2.2 Materials and procedure

The raw material used in the experimental process was obtained from Vital Materials Co., Ltd, with a purity of 6N (99.9999wt%). The raw materials were firstly tested by glow discharge mass spectrometry (GDMS), and the content of each impurity is shown in Table 2. The material mass used for each group of experiments was 4.0 kg, the boat material was quartz, and the length of the quartz was 500 mm. The equipment was produced by Gaomi Putte Electronic Equipment Co., Ltd. The model number was not fixed, as the equipment was customized.

Firstly, 4.0 kg raw material was loaded into a quartz boat, and then put into a vacuum distillation furnace. The experiments were carried out at a distillation temperature of 1073 °C, under a vacuum of 1.0×10^{-4} for 40 h. The experiment's distillation products were obtained at the conclusion.

Subsequently, the refined distillation products were reloaded into a sanitized quartz boat and placed within the zone refining furnace. Zone refining was conducted under the following experimental conditions: five passes of zone refining, a zone movement rate of $30 \text{ mm} \cdot \text{h}^{-1}$, and a nitrogen flow rate of $2 \text{ L} \cdot \text{min}^{-1}$. Nitrogen ventilation was implemented to keep indium from oxidizing while the zone refining process was underway. The zone refining temperature was 250–350 °C. Four melting zones were used for purification in the experimental process, and the length of the melting zones was controlled to be 6–8 cm.

The zone refining process resulted in a high-purity product that was finally hydrogenated. The hydrogenation temperature was 615 °C, the hydrogenation period was 1 h, and the hydrogen flow rate was $2 \text{ L} \cdot \text{min}^{-1}$. The trials were repeated five times under the identical conditions described above, and the outcomes are displayed below.

The hydrogenation process was used to further reduce the volatile impurities in indium metal, while the hydrogen atmosphere protects indium against oxidation during the preparation of indium standard samples. The dimensions of the indium standard sample are 300 mm in length and 40 mm in width.

2.3 Sample detection

The purified sample was removed from the equipment and transferred to a clean bench for sampling. After vacuum distillation, the sample was fused and cast, and then cut with a high-purity titanium tool. After removing the head and tail of the sample after zone refining, the sample in the part near the head and tail was selected. After hydrogenation, the samples were homogeneous and could be sampled directly. Solid samples were analyzed and tested directly by GDMS, and the same batch of samples was tested using the same equipment to ensure the stability of the test. The GDMS analysis technique has the advantages of low risk of contamination in the testing process, strong anti-interference ability, and low detection limit, which enables the analysis of trace elements. The detection limit for most impurities, such as Si, Fe, Ni, Cu, and Zn, is $<0.5 \mu\text{g}/\text{kg}$, and the detection limit of impurities Al, Pb, Bi, Sn, etc. is less than $1.0 \mu\text{g}/\text{kg}$. However, the purity of the current products does not consider the interstitial impurities, such as C, N, O, and H.

3 Results and Discussion

3.1 Purity of indium

The contents of the main impurities in the samples and the purity of indium are shown in Table 3.

Following vacuum distillation, the concentrations of impurities Sn, Pb, and Bi decrease significantly; the concentration of Sb is moderately reduced, though it remains high in the product; the concentration of Fe shows negligible reduction, whereas that of Si increases, potentially due to contamination from the quartz boat during the experiment. It can be seen that during the purification of indium by vacuum distillation technique, the removal of impurities Sn, Pb, and Bi is more effective, followed by impurity Sb, and the removal of impurities Fe and Si is less effective. After vacuum distillation, the purity of indium can be purified from 6N8 to about 7N5.

From the above analysis, it can be seen that after vacuum distillation, the content of impurities Si, Sb, and Fe in the sample is still high. When the sample undergoes zone refining, the contents of impurities Fe and Si are effectively reduced, and the content of impurity Sb is further reduced. The zone refining technique can effectively remove the impurities Fe and Si that cannot be removed during vacuum distillation, and it also has a specific effect on the removal of impurity Sb.

After vacuum distillation and zone refining, most impurities have been effectively removed from the raw indium, and only

Table 2 Impurity content of raw materials (μg/kg)

Al	Si	P	S	Mn	Fe	Bi	Ni	Cu	Zn	Sn	Sb	Pb	Total
<2	11	0.5	1.2	<0.5	5.6	42	4.9	<0.5	0.5	55	56	8.2	184.9

Table 3 Indium purity and impurity content ($\mu\text{g}\cdot\text{kg}^{-1}$)

Element	Al	Si	P	S	Mn	Fe	Ni	Cu	Zn	Sn	Sb	Pb	Bi	In
Raw material	<2	11	0.5	1.2	<0.5	5.6	4.9	<0.5	0.5	55	56	8.2	42	6N8
Exp.1	①	<2	35	0.5	<0.5	<0.5	1.5	<0.5	<0.5	0.5	<2	19	<1	<1
	②	<2	<0.5	<0.5	3.9	<0.5	0.9	<0.5	<0.5	0.5	<2	23	<1	<1
	③	<5	1.1	<0.5	9.2	<0.5	<0.5	1.7	<0.5	0.6	<2	3.3	<1	<1
Exp.2	①	<2	10	<0.5	<0.5	<0.5	5.2	3.5	0.6	<0.5	<2	14	<1	<1
	②	<5	<0.5	<0.5	<0.5	<0.5	<0.5	<0.5	<0.5	0.6	4.2	26	<1	<1
	③	<2	1.3	<0.5	<0.5	<0.5	<0.5	<0.5	<0.5	<0.5	<2	4.1	<1	<1
Exp.3	①	<2	24	<0.5	<0.5	<0.5	3.6	1.1	0.8	<0.5	<2	18	<1	<1
	②	<5	<0.5	<0.5	<0.5	<0.5	<0.5	<0.5	<0.5	<0.5	<2	7.1	<1	<1
	③	<1	3.7	<0.5	0.6	<0.5	1.2	1.1	<0.5	6.1	<2	<1	<1	<1
Exp.4	①	<2	37	<0.5	<0.5	<0.5	8.5	5.7	0.7	<0.5	<2	16	<1	<1
	②	<5	3	<0.5	1.1	0.5	0.6	<0.5	<0.5	<0.5	<2	7.1	<1	<1
	③	<2	2.7	5.7	7.1	0.5	1.1	1.8	<0.5	2.5	<2	3.1	<1	<1
Exp.5	①	<2	20	<0.5	1.6	<0.5	2.2	<0.5	1.2	<0.5	<2	21	<1	<1
	②	<2	1.2	<0.5	<0.5	<0.5	1.8	<0.5	<0.5	<0.5	<2	9.8	<1	<1
	③	<2	<0.5	<0.5	8.8	<0.5	0.7	<0.5	<0.5	0.5	<2	2.5	<1	<1

Note: < indicates that it is below the detection limit of the instrument; ①: vacuum distillation; ②: zone refining; ③: hydrogenation

the content of impurity Sb is still high. After hydrogenation, the contents are all below 5 $\mu\text{g}/\text{kg}$. The purity of the sample can reach 7N8.

Analyzed from Table 3, in five groups of experiments, the experimental conditions are consistent, and the purities are as follows. After vacuum distillation, the purity of the products is 7N4–7N6; after purification by zone refining, the purity of the products in two groups of experiments is 7N7, and the purities of the products in the other three groups of experiments are 7N8, 7N8, and 8N2, separately. After purification by hydrogenation, the purity of the products in three groups of experiments is 7N8, and the purities of the products in the other two groups are 7N7 and 7N9, separately. The purity of one of the samples after zone refining is 8N2, which might be a testing error according to the data analysis. The other test data are relatively stable. This indicates that the repeatability of the experiment and the repeatability of the test are high, and the results of the experiment are scientific.

3.2 Efficiency of impurity removal in different processes

As demonstrated in the preceding analysis, the removal efficiency of impurities varies significantly in different processes. To further investigate the impact of various processes on the elimination of major impurities in indium, a classification of these impurities is presented below for detailed analysis.

3.2.1 Vacuum distillation

After vacuum distillation, the average content and removal efficiency of the main impurities in indium are shown in Fig. 4. The impurities Sn and Bi are reduced from 55 and 42 $\mu\text{g}\cdot\text{kg}^{-1}$ to 2 and 1 $\mu\text{g}\cdot\text{kg}^{-1}$, and the removal efficiencies reach 96.36% and 97.62%, respectively. The removal efficiencies of impurities Pb and Ni are 87.80% and 53.88%, respectively, and the total removal efficiency is 70.81%. The content of impurity Si in the product is higher than that of the raw material, probably due to the distillation product condensing on the quartz tube, which results in Si contamination. The impurity Si can be removed by zone refining.

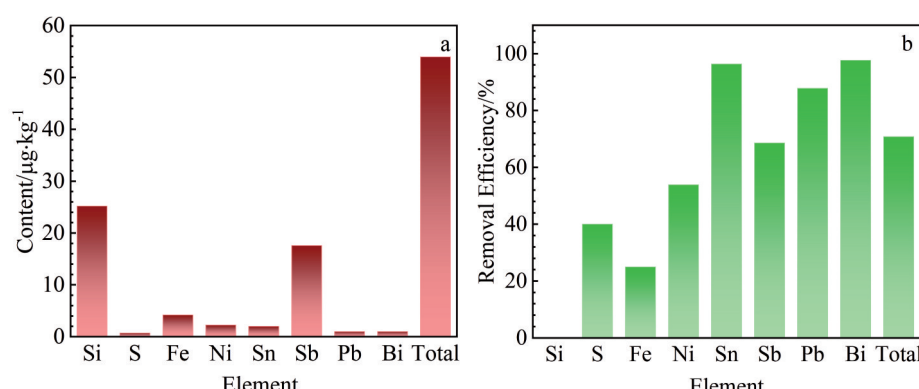


Fig.4 Impurity content (a) and removal efficiency (b) after vacuum distillation

As theoretically analyzed in Section 2.1, using two-stage temperature control is beneficial for removing impurities such as Sn, Pb, and Bi. By controlling the condensation temperature and slowing down the change of temperature gradient in the condensation section, the difficult-to-remove impurities are fully separated, thus improving the removal efficiency of impurities.

The direct recovery ratio of the indium distillation process is shown in Table 4, and the average direct recovery ratio of the indium vacuum distillation is 82.7%.

3.2.2 Zone refining

The average content and removal efficiency of major impurities in indium after zone refining using distillation products as raw materials are shown in Fig. 5. After zone refining, the removal efficiencies of impurities Si, Fe, and Ni reach 95.48%, 79.52%, and 77.88%, respectively, with a total removal efficiency of 57.69%. The content of impurity Sb is further reduced, and the average content decreases to

Table 4 Direct recovery results for the indium distillation process

Experiment	Raw material/kg	Product/kg	Distillation residue/kg	Direct recovery ratio/%
Exp.1	4.0099	3.4771	0.4815	86.7
Exp.2	4.0057	3.1193	0.7531	77.9
Exp.3	3.9981	3.2585	0.5927	81.5
Exp.4	4.0054	3.3491	0.4708	83.6
Exp.5	3.9934	3.3491	0.1411	83.9
Average	4.0025	3.3106	0.4878	82.7

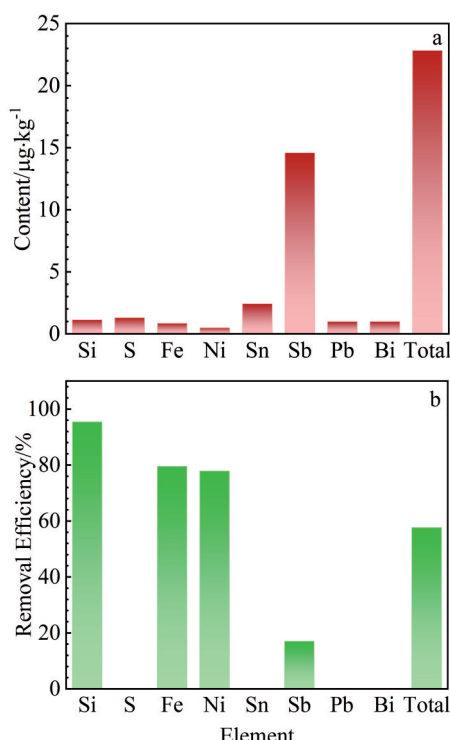


Fig.5 Impurity content (a) and removal efficiency (b) after zone refining

14.6 $\mu\text{g}\cdot\text{kg}^{-1}$.

From the analysis in Section 2.1, it can be seen that the distribution coefficients of impurities Sn, Pb, and Bi are close to 1, so the zone refining process is ineffective in removing them. The distribution coefficients of impurities Si, Fe, and Ni are much less than 1, so the removal efficiency is higher in the zone refining process.

3.2.3 Hydrogenation

The average content and removal efficiency of major impurities in indium after hydrogenation casting using zone refining products as raw materials are shown in Fig. 6. After hydrogenation for ingot casting, the content of impurity Sb is further reduced to 2.8 $\mu\text{g}\cdot\text{kg}^{-1}$ and the total impurity content is 16.72 $\mu\text{g}\cdot\text{kg}^{-1}$, with a total impurity removal efficiency of 26.80%.

Hydrogenation has two main effects. On the one hand, it prevents indium from oxidization during the experiment, and at the same time, it removes oxides from the surface of indium. After hydrogenation, indium has a more metallic luster. On the other hand, after vacuum distillation and zone refining, the content of impurity Sb is still high. The impurity Sb is volatile, and it will be further volatilized during the hydrogenation process, thus improving the removal efficiency of the impurity Sb. It is shown that hydrogenation is beneficial in removing impurities from indium.

3.3 Removal efficiency of impurities

To further analyze the effectiveness of different processes in removing impurities from indium, the following analyses were performed. The removal efficiency of impurities Fe, Sb,

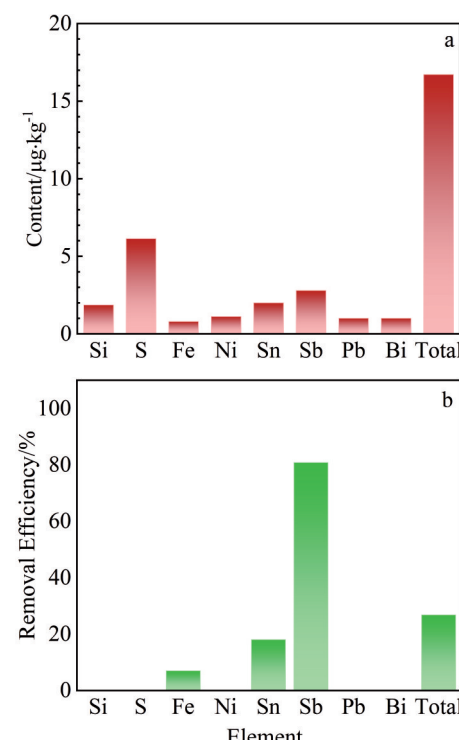


Fig.6 Impurity content (a) and removal efficiency (b) after hydrogenation

Si, and Ni is shown in Fig. 7. As inferred from the figure, elements such as Fe, Sb, Si, and Ni cannot be efficiently removed by vacuum distillation alone, whereas their removal efficiency is significantly improved by subsequent zone refining, especially for Fe, Si, and Ni, which exhibit more pronounced purification enhancement. After the hydrogenation operation again, the removal efficiency of impurity Sb can be further improved, and there is no beneficial effect on impurity Fe, Si, and Ni; on the contrary, the removal efficiency will be reduced. Therefore, for raw indium materials with low impurity Sb content, only vacuum distillation and zone refining processes are required, and hydrogenation again will not benefit the purification of indium metal.

The removal efficiency of impurities Bi, Sn, and Pb is shown in Fig. 8. Vacuum distillation is more effective in removing impurities Bi, Sn, and Pb from indium, and the removal efficiency of impurity is not improved when the samples are subjected to zone refining and hydrogenation operations again. It suggests that if indium mainly contains impurities such as Bi, Sn, and Pb, and the content of other impurities is low, indium can achieve a high purity by the vacuum distillation process alone. When calculating the removal efficiency of impurities, the impurity content below the detection limit is calculated as the detection limit.

The preceding analysis further confirms that effective removal of most impurities is achieved via combined vacuum

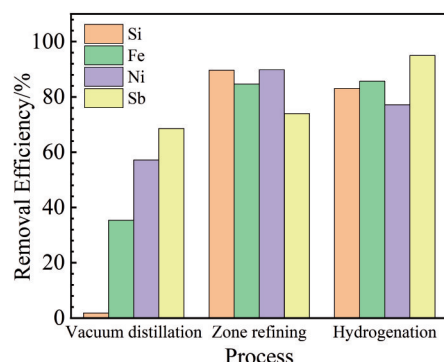


Fig. 7 Removal efficiency of impurities Fe, Sb, Si, and Ni after different processes

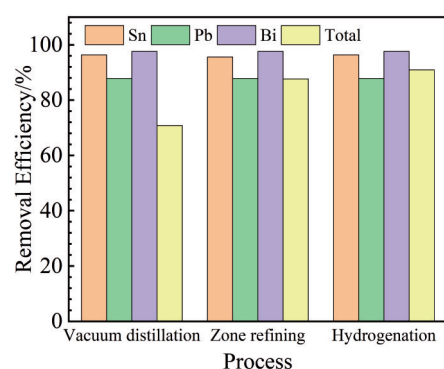


Fig. 8 Removal efficiency of impurities Bi, Sn, and Pb after different processes

distillation and zone refining, yet the concentration of impurity Sb remains notably high. For example, the removal efficiency of impurities Sn and Bi can reach more than 95%, the removal efficiency of impurities Si, Fe, Ni, and Pb can reach more than 85%, while the removal efficiency of impurity Sb is only less than 75%, and the total removal efficiency of impurities is 87.6%. After the hydrogenation process, the impurity Sb can be further removed, and the total removal efficiency of impurities reaches 90.9%.

The final removal efficiency of impurities after vacuum distillation, zone refining, and hydrogenation of indium is shown in Fig. 9. The total impurity content is reduced from 184.9 $\mu\text{g/kg}$ to 10.4 $\mu\text{g/kg}$.

After vacuum distillation, zone refining, and hydrogenation of indium, the contents of impurities Sn, Sb, and Si are reduced from 55.0, 56.0, and 11.0 $\mu\text{g/kg}$ to 2.0, 4.1, and 1.1

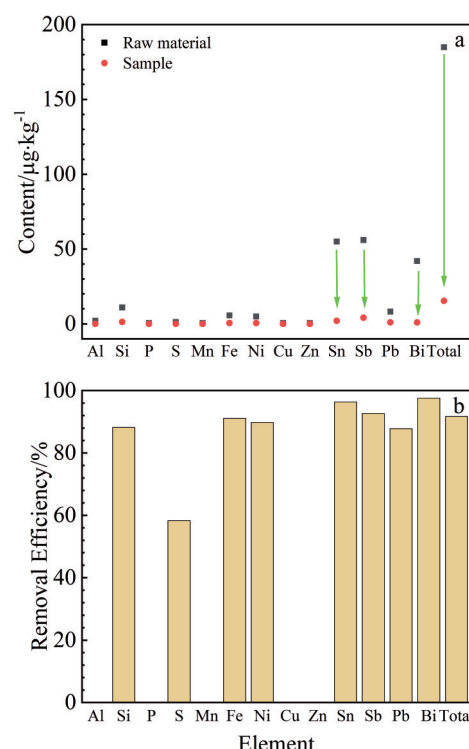


Fig. 9 Final content (a) and removal efficiency (b) of impurities after vacuum distillation, zone refining, and hydrogenation



Fig. 10 Indium products after hydrogenation

Table 5 Comparison of impurity content in samples of industry standards (μg·kg⁻¹)

Element	Standard	Concentration
Ag	2.0	<1.0
Cd	5.0	<5.0
Cu	5.0	<0.5
Fe	5.0	<0.5
Mg	5.0	<0.5
Ni	5.0	<0.5
Pb	10.0	<1.0
Zn	2.0	<0.5
Al	-	<2.0
Au	-	-
Ca	-	<2.0
Co	-	<0.5
V	-	<0.5
Cr	-	<0.5
Ga	-	<5.0
Mn	-	<0.5
Na	-	<0.5
Ti	-	<0.5
Tl	-	<2.0
Total	100	<22.5

μg/kg, with the removal efficiency reaching 96.4% and 92.7%, respectively. The contents of impurities Fe and Ni can be reduced to less than 0.5 μg/kg, with the removal efficiency reaching 90.0%. The contents of impurities Pb and Bi can be reduced to less than 1.0 μg/kg, and the total impurity removal efficiency reaches 91.7%. Fig.10 shows a standard 7N product after hydrogenated ingot casting, which can be sold as a high-end raw material.

Comparison of the impurity content in the sample with the industry standard is shown in Table 5. It can be seen that the purity of the sample meets the 7N indium industry standard.

4 Conclusions

1) Using 6N high-purity indium as raw material, 7N high-purity indium can be successfully prepared by combination of vacuum distillation, zone refining, and hydrogenation process.

2) Following the multi-step purification process, the contents of impurities Sn, Sb, and Si are decreased from 55.0, 56.0, and 11.0 μg/kg to 2.0, 4.1, and 1.1 μg/kg, respectively. Additionally, impurities such as Fe, Pb, Bi, and Ni can be reduced below the instrumental detection limit, with the total impurity content dropping from 184.9 μg/kg to 10.4 μg/kg.

3) The total removal efficiency of impurities reaches 90.9%, and the purity of indium metal reaches 7N9.

Reference

1 Wang X W, Wang W, Chen W et al. *Materials Characterization*[J], 2021, 177: 111157

- 2 Li L B, Li Q, Wang H et al. *Rare Metal Materials and Engineering*[J], 2015, 44(6): 1374
- 3 Kwon Y, Kim S. *NPG Asia Materials*[J], 2021, 13(1): 36
- 4 Zhu Y, He Y L, Jiang S S et al. *Journal of Semiconductors*[J], 2021, 42(3): 27
- 5 Ma X B, Zhang W J, Wang D X et al. *Rare Metal Materials and Engineering*[J], 2015, 44(12): 2937
- 6 Fan Y Y, Liu Y, Niu L P et al. *Separation and Purification Technology*[J], 2021, 269: 118766
- 7 Cojocaru-Mire ' Din O, Choi P, Wuerz R et al. *Ultramicroscopy*[J], 2011, 111: 552
- 8 Wade T L, Vaidyanathan R, Happek U et al. *Journal of Electroanalytical Chemistry*[J], 2001, 500: 322
- 9 Ajayan J, Nirmal D, Ravichandran T et al. *Int J Electron Commun*[J], 2018, 94: 199
- 10 Baek K, Jang K, Lee Y J et al. *Thin Solid Films*[J], 2013, 531: 349
- 11 Zhang H, Wang S, Tian Y H et al. *Nano Materials Science*[J], 2021, 42: 304
- 12 Yu Y, Song J P, Bai F et al. *International Journal of Refractory Metals and Hard Materials*[J], 2020, 2(2): 164
- 13 Chen L L, Wang Y N, Kong L X et al. *Journal of Materials Research and Technology*[J], 2024, 28: 1382
- 14 Zhang X W, Wang Z Q, Chen D H et al. *Rare Metal Materials and Engineering*[J], 2016, 45(11): 2793
- 15 Li Z C, Chen Z J, Ma W H et al. *Vacuum*[J], 2024, 221: 112884
- 16 Lei Haocheng, Deng Yong, Liu Dachun et al. *Journal of Kunming University of Science and Technology (Natural Science)*[J], 2019, 44(5): 8 (in Chinese)
- 17 Zhu Enwen, Chen Yinghong. *World Nonferrous Metals*[J], 2018, 11: 168 (in Chinese)
- 18 Zhang Dingchuan, Deng Yong, Yuan Congcong et al. *Chinese Journal of Vacuum Science and Technology*[J], 2017, 37(1): 94 (in Chinese)
- 19 Wang Y B, Jin Q L, Duan X Y et al. *Vacuum*[J], 2023, 217: 112557
- 20 Tian Q H, He Z Q, Xu Z P et al. *Metallurgical and Materials Transactions B*[J], 2024, 55(2): 772
- 21 Yu L, Kang X A, Chen L N et al. *Materials*[J], 2021, 14(8): 2064
- 22 Roussopoulos G S, Rubini P A. *Journal of Crystal Growth*[J], 2004, 271(3-4): 333
- 23 Huang J, Ren Q B, Hu Z Q et al. *Rare Metal Materials and Engineering*[J], 2017, 46(12): 3633
- 24 Wu Meizhen, Zhang Chunjing. *Mining & Metallurgy*[J], 2016, 25(1): 59 (in Chinese)
- 25 Prasad D S, Munirathnam N R, Rao J V et al. *Materials Letters*[J], 2006, 60(15): 1875
- 26 Munirathnam N R, Prasad D S, Rao J V et al. *Indian Academy of Sciences*[J], 2005, 28(4): 309
- 27 Zha G Z, Yang C F, Wang Y K et al. *Separation and Purification Technology*[J], 2019, 209: 863

28 Cheng K K, Yi J F, Zha G Z et al. *Separation and Purification Technology*[J], 2022, 278: 119531

29 Dai Yongnian, Zhao Zhong. *Vacuum Metallurgy*[M]. Beijing: Metallurgical Industry Press, 1988 (in Chinese)

30 Li D S, Dai Y N, Yang B et al. *Journal of Central South University*[J], 2013, 20(3): 337

31 Pfann W G. *JOM*[J], 1955, 7: 297

32 Pfann W G. *JOM*[J], 1952, 4(7): 747

33 Huan Z, Zhao J Y, Xu J J et al. *Russian Journal of Non-ferrous Metals*[J], 2020, 61(1): 9

34 Pfann W G. *Metallurgical Reviews*[J], 1957, 2(1): 29

35 Lan C W. *International Journal of Heat and Mass Transfer*[J], 2000, 43: 1987

36 Zhang X X, Friedrich S, Friedrich B. *Metals*[J], 2021, 11(2): 201

37 Duan M P, Zhao J Y, Xu B Q et al. *Transactions of Nonferrous Metals Society of China*[J], 2023, 33: 2843

38 Deng Yong, Li Dongsheng, Yang Bin et al. *Chinese Journal of Vacuum Science and Technology*[J], 2014, 34(7): 754 (in Chinese)

39 Wan H L, Xu B Q, Yang B et al. *Vacuum*[J], 2020, 171: 108839

40 Zhang X X, Friedrich S, Friedrich B. *Journal of Crystallization Process and Technology*[J], 2018, 8(1): 33

真空蒸馏-区域熔炼联合法制备7N高纯铟

田庆华¹, 胡智向^{1,2}, 何志强¹, 郭学益¹, 朱 刘², 许志鹏¹

(1. 中南大学 冶金与环境学院, 湖南 长沙 410083)

(2. 先导稀材股份有限公司, 广东 清远 511500)

摘要: 高纯铟广泛应用于航空航天、电子、医疗、能源和国防领域。铟的纯度和杂质含量对这些应用有着重要影响。采用真空蒸馏和区域熔炼相结合的方法制备了高纯铟。结果表明, 杂质Sn和Bi的去除率超过95%, 杂质Sb的平均去除率接近95%, Si、Fe、Ni和Pb的去除率超过85%。最终, 杂质Sn和Sb分别降低至2.0和4.1 μg/kg, Fe、Ni、Pb和Bi等多数杂质含量均降低至仪器检测限以下。总体杂质去除率为90.9%, 铟纯度达到7N9。

关键词: 铟; 高纯; 真空蒸馏; 区域精炼

作者简介: 田庆华, 男, 1981年生, 博士, 教授, 中南大学冶金与环境学院, 湖南 长沙 410083, E-mail: qinghua@csu.edu.cn